



*Supplement of*

## **Satellite observations of smoke–cloud–radiation interactions over the Amazon rainforest**

**Ross Herbert and Philip Stier**

*Correspondence to:* Ross Herbert ([ross.herbert@physics.ox.ac.uk](mailto:ross.herbert@physics.ox.ac.uk))

The copyright of individual parts of the supplement might differ from the article licence.

The supplementary material consists of eight additional figures (Figures S1 to S8) to support text in the manuscript, and a table detailing the variables extracted from the satellite data products (Table S1).

## Figures S1 to S8

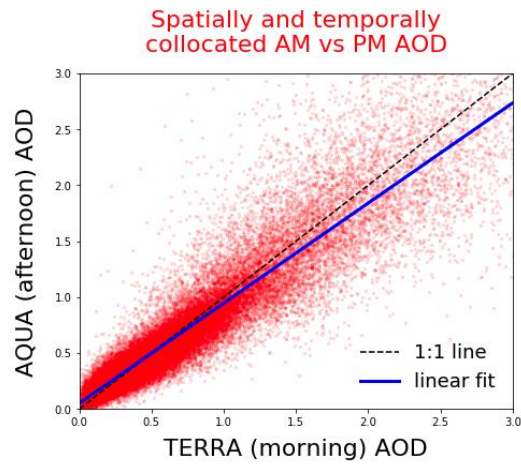


**Figure S1.** Comparing the morning and afternoon AOD retrievals over the Amazon from the MODIS instrument. Each red dot shows the spatially collocated data (1 degree) from the two overpasses for each day of the timeseries. The black dashed line shows the 1:1 line and the solid blue line shows the linear regression of the full dataset.

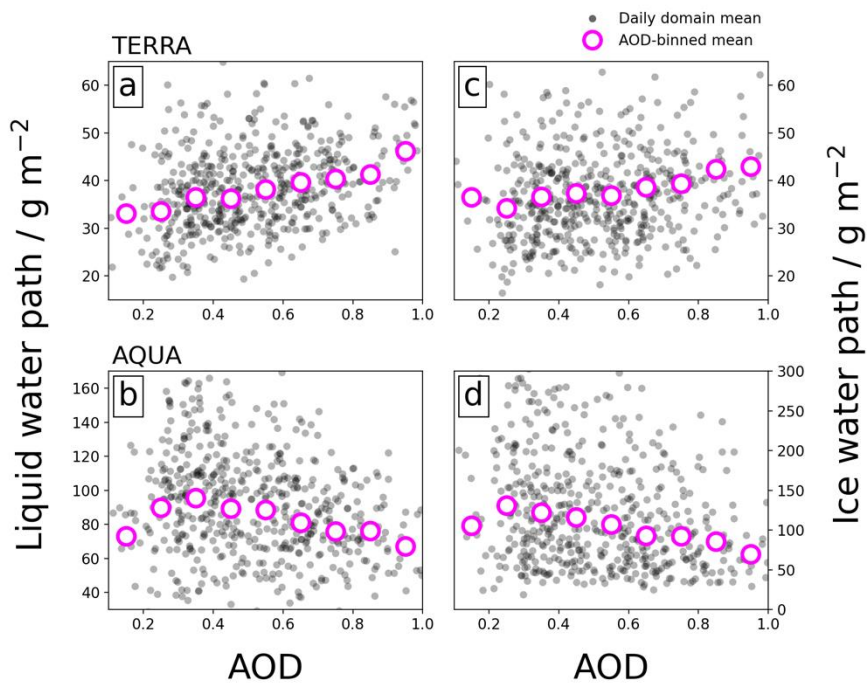


**Figure S2.** Domain mean LWP (a and b) and IWP (c and d) as a function of AOD for the TERRA overpass (top row) and AQUA overpass (bottom row). The grey filled circles show the data for each day of the timeseries and the empty magenta circles show the mean of all days binned by AOD.

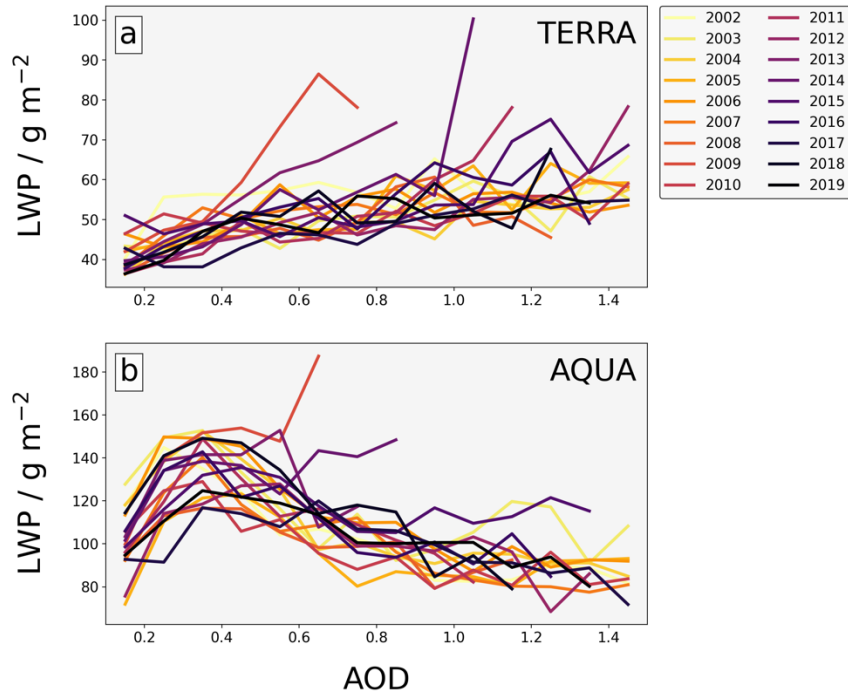


**Figure S3.** Geometric mean LWP as a function of binned AOD for each year of the timeseries (2002 to 2019) for the morning TERRA (a) and AQUA (b) overpasses.

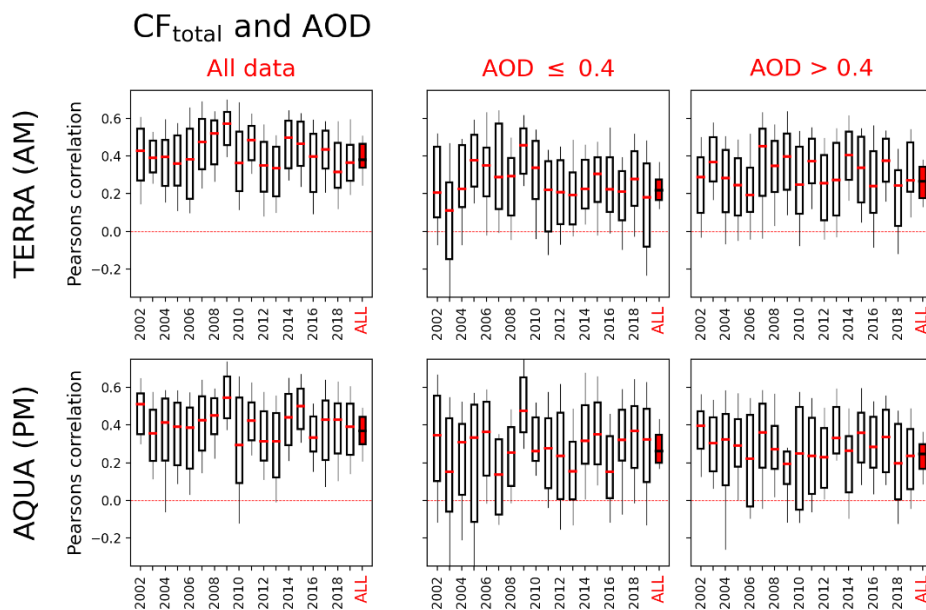


**Figure S4.** Boxplots showing Pearson's correlation coefficients in the domain, for each year of the timeseries. Right-most boxplots (in red) in each subplot shows the data for all years. Pearson's correlation coefficient between  $CF_{total}$  and AOD. Top row shows the TERRA overpass in the AM, and lower row shows the AQUA overpass in the PM. Left column shows the spatial distribution of the coefficient for all data, middle column shows data for  $AOD \leq 0.4$ , and right column shows data for  $AOD > 0.4$ . Red colours depict a positive correlation, blue colours a negative correlation.

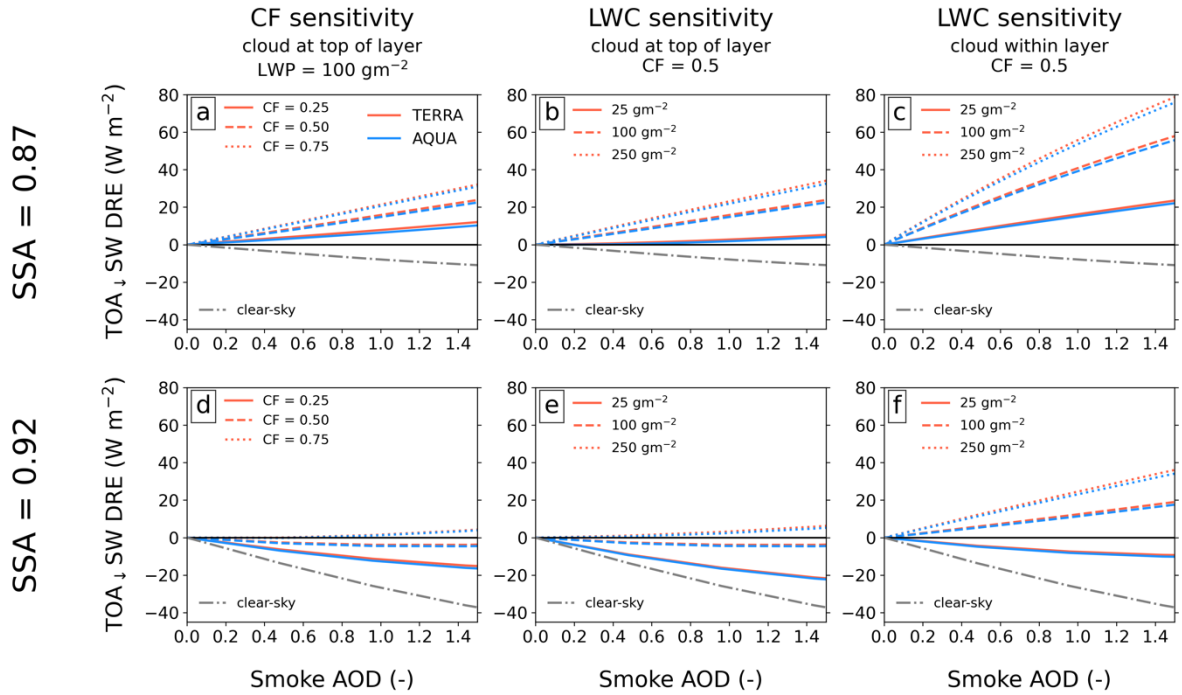


**Figure S5.** Instantaneous all-sky shortwave aerosol direct effect (DRE) at TOA as function of smoke AOD in an offline 1D radiative transfer model (ecRad; Hogan and Bozzo, 2018). The DRE is shown for typical variations in cloud fraction (a and d), liquid-water content for a single cloud at the top of the aerosol layer (b and e), and liquid-water content for a single cloud within the aerosol layer (d and f). Red and blue lines show calculations for TERRA and AQUA overpass times, and the grey dot-dash line shows the clear-sky DRE. The top row (a – c) shows calculations assuming an SSA of 0.87, and the bottom row (d – f) assuming an SSA of 0.92, thereby spanning commonly observed smoke SSA across the region.

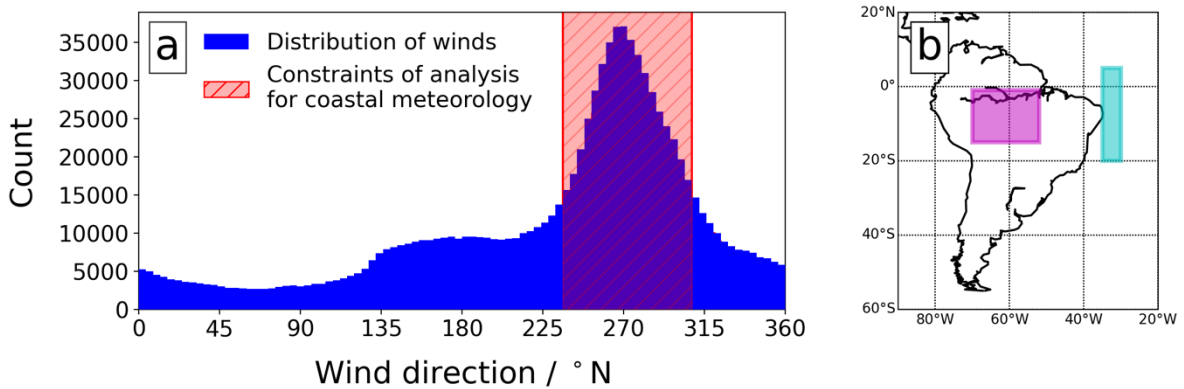


**Figure S6.** Plot (a) shows the distribution of ERA5 1-degree winds collocated with the satellite data analysis. The red hatched section constitutes the 50% of the most frequent wind direction. Plot (b) shows the extents of the analysis domain (magenta) and the coastal domain (cyan). The coastal domain over the eastern coast of the continent is used to determine the mean meteorological conditions upstream of the easterlies that pass over the analysis region.

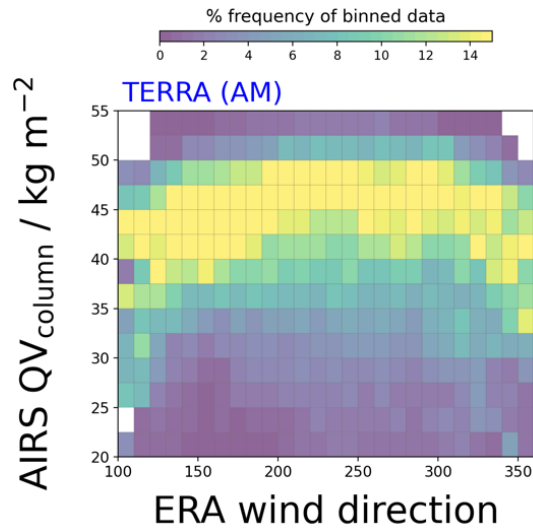


**Figure S7.** Joint histograms showing the % frequency of daily mean AIRS total column water vapour as a function of collocated ERA wind direction in the analysis region.

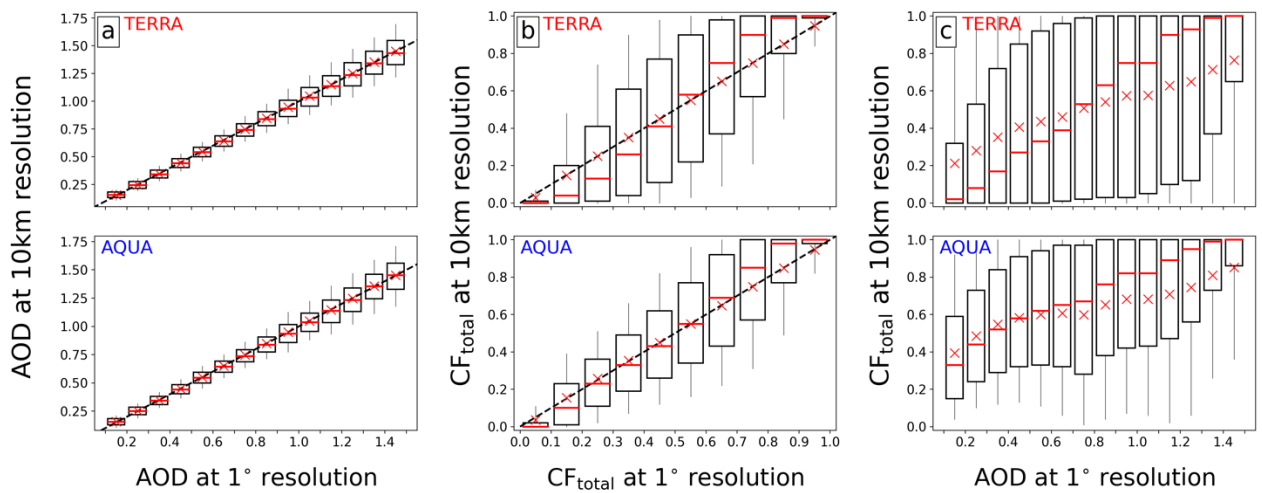


**Figure S8.** Comparing total cloud fraction ( $CF_{total}$ ) and aerosol optical depth (AOD DT+DB) from MODIS level 2 products (5-km for  $CF_{total}$ ; 10-km for AOD) and level 3 products (1 degree resolution). Fine resolution data is binned by the coarse resolution data and displayed as a boxplot (red bar shows median; red cross shows mean). The comparisons are shown for (a) AOD, (b)  $CF_{total}$ , and (c) for  $CF_{total}$  at 10-km and AOD at 1 degree. Top row is for the TERRA overpass, and the bottom row for the AQUA overpass.

## Tables

**Table S1.** Satellite and reanalysis datasets and variables used in the analysis.

Dataset source	Variable name in dataset	Short name
<b>MODIS:</b>	AOD_550_Dark_Target_Deep_Blue_Combined_Mean	AOD
TERRA_MYD08_D3 and AQUA_MYD08_D3	Cloud_Fraction_Day_Mean	CF <sub>total</sub>
	Cloud_Retrieval_Fraction_Liquid	CF <sub>liquid</sub>
	Cloud_Optical_Thickness_Combined_Mean	COT <sub>total</sub>
	Cloud_Optical_Thickness_Liquid_Mean	COT <sub>liquid</sub>
	Cloud_Top_Temperature_Day_Mean	CTT
	Cloud_Top_Height_Day_Mean	CTH
	Cloud_Water_Path_Liquid_Mean	LWP
	Cloud_Water_Path_Ice_Mean	IWP
	Cirrus_Fraction_SWIR	CF <sub>cirrus</sub>
	Cloud_Effective_Radius_Liquid_Mean	RE <sub>liquid</sub>
<b>ERA5</b> reanalysis	ta (850 hPa temperature)	T <sub>850</sub>
	hus (850 hPa specific humidity)	QV <sub>850</sub>
	ua (850 hPa U wind component)	U <sub>850</sub>
	va (850 hPa V wind component)	V <sub>850</sub>
	tas (Surface temperature at 2m)	T <sub>2m</sub>
<b>CERES:</b>	toa_sw_all_1h (TOA shortwave flux)	SW <sub>TOA</sub>
SSF1deg_1H_Aqua_MODIS_4.1 and SSF1deg_1H_Terra_MODIS_4.1	toa_lw_all_1h (TOA longwave flux)	LW <sub>TOA</sub>
	toa_net_all_1h (TOA net flux)	NET <sub>TOA</sub>
	toa_solar_all_1h (TOA solar flux)	SOL <sub>TOA</sub>
<b>IMERG:</b>		
3B-DAY_MS_MRG_3IMERG_V06	precipitationCal (Mean daily accumulated precipitation)	P <sub>accum</sub>
3B-HHR_MS_MRG_3IMERG_V06B	precipitationCal (Instantaneous precipitation rate)	P <sub>AM</sub> , P <sub>PM</sub> , P <sub>peak</sub>
<b>AIRS:</b>		
L3_RetStd_IR001_v7	H2O_MMR_Surf_TqJ_A (Surface water vapour MMR)	QV <sub>surface</sub>
	RelHumSurf_liquid_TqJ_A (Surface relative humidity)	RH <sub>surface</sub>
	TotH2OVap_TqJ_A (Total column water vapour)	QV <sub>column</sub>
<b>MODIS 1/5km cloud product:</b>		
MOD06_L2 and MYD06_L2	Cloud Top Height	CTH <sub>10km</sub>
	Cloud Top Temperature	CTT <sub>10km</sub>
	Cloud Fraction	CF <sub>10km</sub>
	Cloud Effective Radius	RE <sub>10km</sub>
	Cloud Optical Thickness	COT <sub>10km</sub>
	Cloud Water Path	CWP <sub>10km</sub>
<b>MODIS 10km aerosol product:</b>		
MOD04_L2 and MYD04_L2	AOD_550_Dark_Target_Deep_Blue_Combined	AOD <sub>10km</sub>

## References

Hogan, R. J. and Bozzo, A.: A Flexible and Efficient Radiation Scheme for the ECMWF Model, *Journal of Advances in Modeling Earth Systems*, 10, 1990–2008, <https://doi.org/10.1029/2018MS001364>, 2018.